PAPER • OPEN ACCESS

Non-adiabatic generation of NOON states in a Tonks–Girardeau gas

To cite this article: James Schloss *et al* 2016 *New J. Phys.* **18** 035012

New Journal of Physics
The open access journal at the forefront of physics

Deutsche Physikalische Gesellschaft DPG
IOP Institute of Physics

Published in partnership with: Deutsche Physikalische Gesellschaft and the Institute of Physics

OPEN ACCESS

RECEIVED
29 December 2015

REVISED
1 March 2016

ACCEPTED FOR PUBLICATION
3 March 2016

PUBLISHED
22 March 2016

PAPER

Non-adiabatic generation of NOON states in a Tonks–Girardeau gas⋆

James Schloss, Albert Benseny, Jérémie Gillet, Jacob Swain and Thomas Busch

Quantum Systems Unit, Okinawa Institute of Science and Technology, 904-0495 Okinawa, Japan

E-mail: james.schloss@oist.jp

Keywords: NOON states, optimal control, quantum engineering, strongly correlated quantum states, shortcuts to adiabaticity, Tonks–Girardeau gas

Abstract

Adiabatic techniques can be used to control quantum states with high fidelity while exercising limited control over the parameters of a system. However, because these techniques are slow compared to other timescales in the system, they are usually not suitable for creating highly unstable states or performing time-critical processes. Both of these situations arise in quantum information processing, where entangled states may be isolated from the environment only for a short time and where quantum computers require high-fidelity operations to be performed quickly. Recently it has been shown that techniques like optimal control and shortcuts to adiabaticity can be used to prepare quantum states non-adiabatically with high fidelity. Here we present two examples of how these techniques can be used to create maximally entangled many-body NOON states in one-dimensional Tonks–Girardeau gases.

1. Introduction

Macroscopic superposition states, such as the maximally entangled $|N,\,0\rangle + |0,\,N\rangle$ (NOON) state, are of great interest for fundamental studies of quantum mechanics and for applications in quantum information and quantum metrology. A NOON state is composed of two modes where all particles in the system can be found exclusively in either one or the other. Until now, experimental NOON state generation has been limited to photonic states generated by mixing classical states with down-converted photon pairs [1], and with such techniques it has been possible to create NOON states with around five photons [2]. A theoretical proposal for an experimentally realistic setup for creating NOON states for a large number of ultracold atoms was recently presented by Hallwood *et al* [3], who considered a gas of strongly interacting bosons in a one-dimensional ring. In this proposed system, different angular momentum states were coupled by breaking the rotational symmetry, and the authors showed how to accelerate the atoms into a superposition state of rotating and non-rotating components. Since the atoms were considered to be in the strongly correlated (Tonks–Girardeau) regime [4], this process results in a macroscopically entangled state.

In order to successfully generate NOON states on a ring of strongly correlated ultracold atoms, it is crucial to rotationally accelerate the system slowly, as otherwise unwanted excitations may drive the system out of the desired state. This is especially important close to the avoided crossings where the NOON state lives and where states with different angular momentum quantum numbers are coupled. For larger particle numbers and finite width coupling barriers, the energy gaps at these positions become exponentially small [5], and therefore slower and slower driving is necessary. However, slow processes are not particularly suitable for applications in quantum information, where algorithms must be performed quickly, or for creating states that are highly unstable. Techniques which can speed up the creation process while maintaining high fidelities are therefore of large interest.

Here we present two examples of such techniques that can accelerate the technique for NOON-state preparation suggested by Hallwood *et al* [3]. The first is the chopped random basis (CRAB) optimal control

⋆ Dedicated to the memory of Marvin D Girardeau.

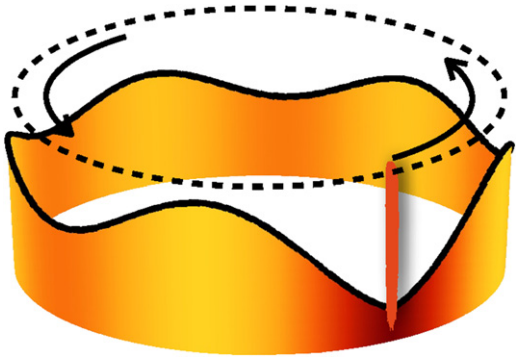

Figure 1. Schematic of the system described by Hallwood *et al* [3]. Shown is the density profile for five atoms in the TG regime which are stirred by a highly localised potential (indicated by the vertical line).

technique [6], where we numerically optimise the angular acceleration and the height of a barrier. The second technique combines two well-known shortcuts to adiabaticity (STA) protocols [7] which we adapt to the ring geometry. In both cases we show that it is possible to drive the system into a NOON state on timescales much faster than required by adiabaticity.

The paper is organised as follows: in section 2 we briefly review the ring system of strongly correlated ultracold atoms. This is followed in section 3 by a detailed description of how to use the optimal control CRAB algorithm to create NOON states non-adiabatically and in section 4 we show how STA can be used to create the same NOON state with high fidelity in a similar system. We finish with the conclusions in section 5.

2. Creating a NOON state on a ring

Let us begin by briefly summarising the protocol suggested by Hallwood *et al* [3] for creating a NOON state in a gas of strongly correlated bosons. For this we consider a gas of N interacting bosons of mass m on a one-dimension ring with circumference L, similar to ring systems previously introduced in literature [8, 9]. This system includes a potential barrier, modelled by a Dirac δ function, that rotates with an angular frequency Ω (see schematic in figure 1). In the rotating frame, the Hamiltonian of the system is given by [3]

$$H^{(N)} = \sum_{i=1}^{N}\left[\frac{1}{2}\left(-\mathrm{i}\frac{\partial}{\partial x_i} - \Omega\right)^2 + b\delta(x_i) + g\sum_{i<j}^{N}\delta(x_i - x_j)\right], \tag{1}$$

where b is the height of the barrier (in units of $\hbar^2/mL^2$), $x_i \in [-1/2,\ 1/2]$ is the position of the i–th particle (in units of L) and g (in units of $\hbar^2/mL^2$) is the effective interaction strength between the atoms.

In the strongly correlated Tonks–Girardeau (TG) limit ($g \to \infty$), the Hamiltonian $H^{(N)}$ can be solved by using the Bose–Fermi mapping theorem [10, 11], which requires replacing the interaction terms in the Hamiltonian with a boundary condition on the many-body bosonic wavefunction

$$\Psi_{\mathrm{B}}(x_1, x_2, \ldots, x_N) = 0, \qquad \text{if} \qquad x_i - x_j = 0 \quad \text{with} \quad i \neq j. \tag{2}$$

In this so-called hard-core limit, two bosons cannot be at the same point in space, which is formally similar to the Pauli principle for fermions. The Bose–Fermi mapping theorem therefore allows us to replace strongly interacting bosons by non-interacting fermions, for which the many-body wavefunction can be calculated as

$$\Psi_{\mathrm{F}}(x_1, x_2, \ldots, x_N) = \frac{1}{\sqrt{N}}\det\left[\psi_n(x_j)\right]_{n,j=1}^{N}. \tag{3}$$

Here the $\psi_n(x_j)$ are the single particle eigenstates of the trapping potential V_0. However, as the fermionic many-body wavefunction is an antisymmetric function, it needs to be symmetrised to describe the bosonic states by

$$\Psi_{\mathrm{B}}(x_1, x_2, \ldots, x_N) = \prod_{i<j}\ \mathrm{sgn}(x_i - x_j)\Psi_{\mathrm{F}}(x_1, x_2, \ldots, x_N). \tag{4}$$

Calculating the time evolution of the entire strongly interacting gas therefore only requires evolving single-particle states, which are governed by the laboratory-frame Hamiltonian

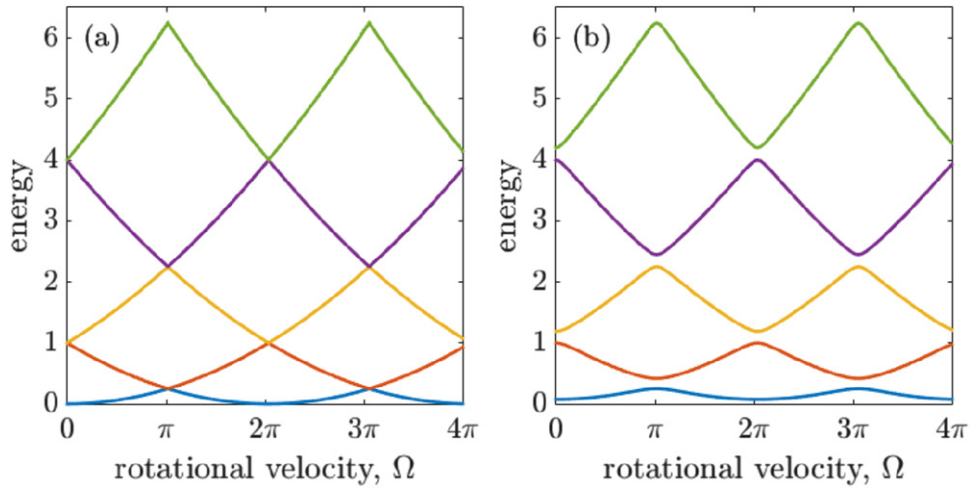

Figure 2. Single particle energy spectrum as a function of Ω for a barrier height of (a) $b = 0$ and (b) $b = 2$. The presence of the barrier leads to the appearance of avoided crossings at intervals of π, which grow in size as a function of barrier height. The degenerate eigenstates for $b = 0$ when Ω is a multiple of 2π correspond to clockwise and counterclockwise rotating plane waves.

$$H = -\frac{1}{2}\frac{\partial^2}{\partial x} + b\delta[x - x_0(t)], \tag{5}$$

where x_0 is the position of the barrier at time t.

The energy spectrum of this system is shown in figure 2 as a function of the rotational velocity $\Omega \equiv \dot{x}_0/L$ (in units of $\hbar/mL$) of the system. In the absence of barrier, $b = 0$ (figure 2(a)), the eigenstates of H are plane waves with quantised angular momentum in units of integer multiples of 2π and manifolds of fixed angular momentum are uncoupled due to the existence of rotational symmetry. However, when $b > 0$ (figure 2(b)) this symmetry is broken and transitions between different manifolds become possible [12], resulting in the avoided crossings visible in the energy spectrum.

By adiabatically accelerating the barrier from $\Omega = 0$ to π, a particle initially in an eigenstate of H will enter a superposition state of two angular momentum eigenstates, and in the TG limit, where the strongly correlated many-particle wavefunction can be directly calculated from the single particles ones, this will create a macroscopic NOON state between different values of angular momentum [3]. However, any non-adiabatic behaviour will lead to transitions to higher or lower lying states in the vicinity of the gaps which would degrade the fidelity of the superposition state. The condition for adiabaticity of the system must therefore be chosen with respect to the smallest gap size, which in general decreases exponentially for higher energies [13]. For a delta barrier, however, the gap size can be shown to stay constant to first order [5].

From an experimental standpoint it would be desirable if the restrictions set by the adiabatic condition could be avoided, and in the following we discuss two strategies with which this can be achieved. The first one makes use of an optimal control technique, which determines an optimal form ('pulse') of the non-adiabatic rotational velocity $\Omega(t)$ which will generate the desired final state with high fidelity through brute-force computational methods. For this we have implemented the CRAB optimal control technique [6], which starts by initially assuming a constant acceleration of the angular barrier velocity from $\Omega = 0$ to π and iterates on this by including procedurally generated sinusoidal variations. After each iteration, the fidelity is calculated and the Nelder–Mead method [14] is used to find the pulse that gives a final state closest to the desired one. This ultimately leads to a form of the rotational velocity that maximises the fidelity for reaching the NOON state in a preset amount of time. In a similar way, we also find optimal pulses for the barrier height, and for a combination of both, the rotational velocity and the barrier height.

The second strategy we consider combines two known results from the area of STA [7]. In order to implement these, we assume that a harmonic or sinusoidal potential can be raised along the perimeter of the ring, and then split the acceleration process into two processes: a first one which breaks the rotational symmetry (raising of a potential), and a second which accelerates the atoms. In order to maximise the fidelity for reaching the NOON state, the rotational symmetry is restored by lowering the potential at the end. It is worth mentioning that a fast quasi-adiabatic shortcut for creating a TG gas superposition state as described above was recently suggested [15].

To quantify the success of our protocols, we use the fidelity $F = |\langle\psi|\phi\rangle|^2$, where $|\psi\rangle$ is the achieved state and $|\phi\rangle$ is the target state. When F is close to one, it is convenient to also define the *infidelity* as $1 - F$. The fidelity between two many-particle TG states, $|\Psi\rangle$ and $|\Phi\rangle$, can be calculated by using the mode by mode projections

[16, 17]

$$\langle\Psi|\Phi\rangle = \frac{1}{N!}\sum_{\eta,\mu\in P}\epsilon_\eta\epsilon_\mu\langle\psi_{\eta_1}(x_1)|\phi_{\mu_1}(x_1)\rangle\cdots\langle\psi_{\eta_N}(x_N)|\phi_{\mu_N}(x_N)\rangle$$
$$= \det[\langle\psi_i|\phi_j\rangle]_{i,j=1}^{N} \tag{6}$$

which follows directly from the form of the TG state [4]

$$\Psi(x_1, x_2, \ldots, x_N) = \frac{1}{\sqrt{N!}}\prod_{i<j}\mathrm{sign}(x_i - x_j)\sum_{\eta\in P}\epsilon_\eta\psi_{\eta_1}(x_1)\cdots\psi_{\eta_N}(x_N). \tag{7}$$

Here P represents the set of all permutations of N elements, ϵ_η represents the antisymmetric tensor of the permutation η, and ψ_i represent the orbitals. These definitions will be used to measure how close the final state of our finite-time algorithms comes to the perfect NOON state.

3. Optimal control

To examine the possibility for using an optimal control approach to generate a NOON state for the TG gas on the ring, we have implemented the CRAB optimal control algorithm [6] for systems of up to five particles. The CRAB technique works by modifying a control parameter of a given system, Γ, with a multiplicative term as

$$\Gamma^{\mathrm{CRAB}}(t) = \Gamma^0(t)\gamma(t), \tag{8}$$

where $\Gamma^0(t)$ is an initial guess, and the function $\gamma(t)$ is written as a sum of $2J$ sinusoidal functions

$$\gamma(t) = 1 + \frac{1}{\lambda(t)}\sum_{j=1}^{J}(A_j\sin(\nu_j t) + B_j\cos(\nu_j t)). \tag{9}$$

To ensure that $\Gamma^{\mathrm{CRAB}}(t)$ and $\Gamma^0(t)$ coincide at the initial and final times, $\lambda(t)$ is defined such that $\lim_{t\to 0}\lambda(t) = \lim_{t\to T}\lambda(t) = \infty$. In our implementation we chose

$$\lambda(t) = \frac{T^2}{4t(t-T)}. \tag{10}$$

The optimisation process then reduces to finding the optimal values for $\{A_j, B_j, \nu_j\}$, which can be achieved by initially assigning random values and then numerically maximising the fidelity by using an algorithm such as the Nelder–Mead method [14]. While it is clear that this process will lead to more accurate outcomes for larger J, the fact that the maximisation has to be carried over a larger number of degrees of freedom also increases the computational complexity. In our case, $\Gamma(t)$ can be chosen to be the rotational angular frequency or the barrier height, which means that we may optimise over the rotation frequency while keeping the barrier height constant, optimise over the barrier height while keeping the rotation acceleration constant, or optimise over both of them simultaneously. These three possibilities will be discussed in the following.

3.1. Optimising over the rotational velocity

Before we discuss the optimal pulse for the full TG, we will focus on the acceleration of a single particle, initially in the ground state of the trap. For this we assume a fixed barrier height and start with a guess pulse that increases linearly from $\Omega = 0$ to π in a preset total time T. The results for $J = 15$ and for $T = 1, 10$, and 100 are shown in figure 3(a). For longer evolution times, a linear pulse is a reasonable method to adiabatically generate the macroscopic superposition state with high fidelity and the modifications stemming from the optimal control process for $T = 100$ can be seen to be weak in magnitude. Shorter evolution times, however, require pulse shapes that strongly influence the system and which therefore differ dramatically from the initial linear guess. From the infidelities for the linear guess pulse and the optimised pulse, shown in figure 5, one can see an improvement of several orders of magnitude on all timescales.

3.2. Optimising over the barrier height

To optimise over the barrier height, we choose a guess pulse which is constant at $b = 1$ while the rotational velocity of the barrier is set to increase linearly from $\Omega = 0$ to π over a total time T. The optimised pulses for the barrier heights for $T = 1, 10$, and 100 for $J = 15$ are shown in figure 3(b), and, similar to the case of varying Ω, shorter evolution times require larger deviations from the initial guess. As in the previous case, these pulses also lead to significant improvements in the final fidelity, shown in figure 5.

3.3. Optimising over rotational velocity and barrier height

With the CRAB algorithm, it is possible to optimise over multiple parameters at the same time. In figure 4, we show the optimal pulses for simultaneously changing the rotational velocity and barrier height. Compared to the

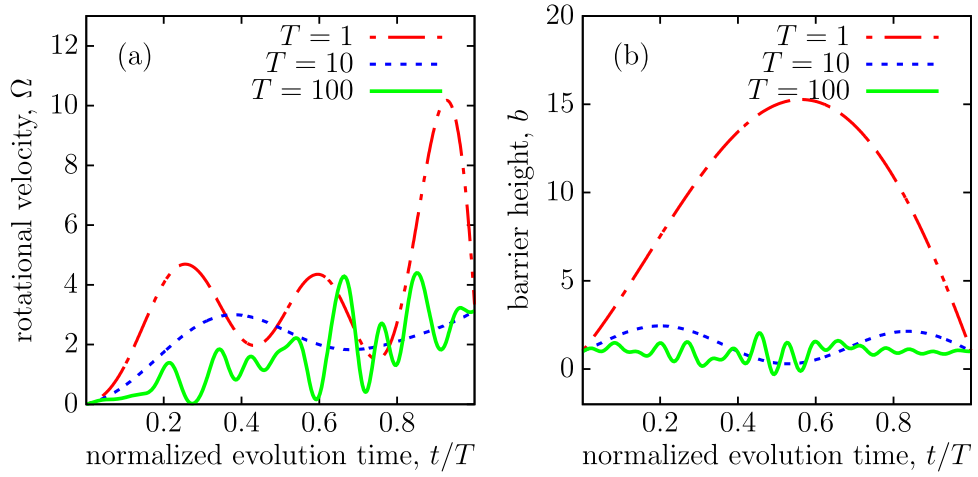

Figure 3. Accelerating a single particle initially in the ground state of the trap. (a) Optimal rotational velocity pulses for $T = 1, 10$, and 100 for fixed barrier height $b = 1$. (b) Optimised barrier height for a linearly increasing rotational velocity, $\Omega = \pi t/T$ for $T = 1, 10$, and 100.

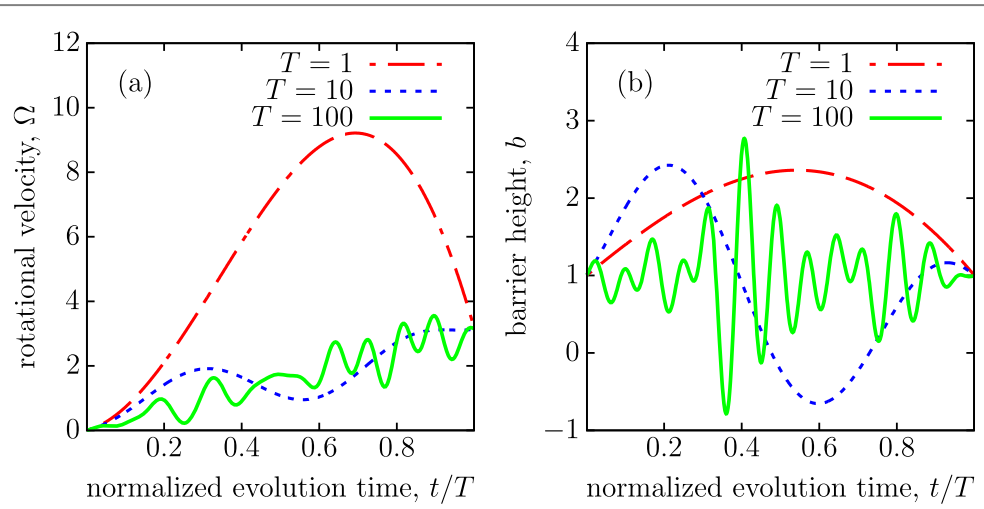

Figure 4. Optimal pulses to accelerate a single particle initially in the ground state of the trap for $T = 1, 10$, and 100 for the (a) rotational velocity and (b) barrier height when optimising over both simultaneously.

previous cases, where only one parameter was optimised, one can see that for longer evolution times the resulting pulse shapes are similar. For shorter times, they differ significantly (compare the red lines in figures 3 and 4). However, the final fidelity is not drastically different from the one stemming from optimising only over the rotation of the barrier (see Figure 5), which is of interest when considering experimental realisations.

3.4. TG gas acceleration

Due to the Bose–Fermi mapping theorem, the evolution of an N-particle TG gas can be calculated by evolving a gas of N spin-polarised independent fermions. Here we only consider the zero temperature limit, in which the fermions in the initial and the target state create a Fermi sea by filling the lowest N energy levels. During the dynamics the atoms close to the Fermi edge can make transitions into empty states, which will affect the global fidelity, and it is therefore most crucial to optimise the dynamics of the overall gas with respect to the particle with the highest energy [15]. In figure 6 we show the fidelity for both, the particle closest to the Fermi edge and the entire TG gas (for $N = 3$ and 5), and one can see that that CRAB algorithm used in this way gives highly effective pulses. Note however, that for very short and long evolution times no significant fidelity increase due to the CRAB algorithm exists for a TG gas.

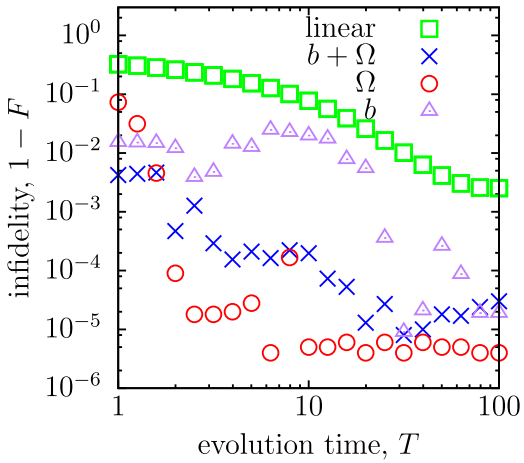

Figure 5. Infidelities as a function of the overall process time for optimally controlled rotational acceleration, barrier height, or both. Here, 'linear' refers to an unoptimised linear acceleration from $\Omega = 0$ to π while keeping the barrier height fixed at $b = 1$.

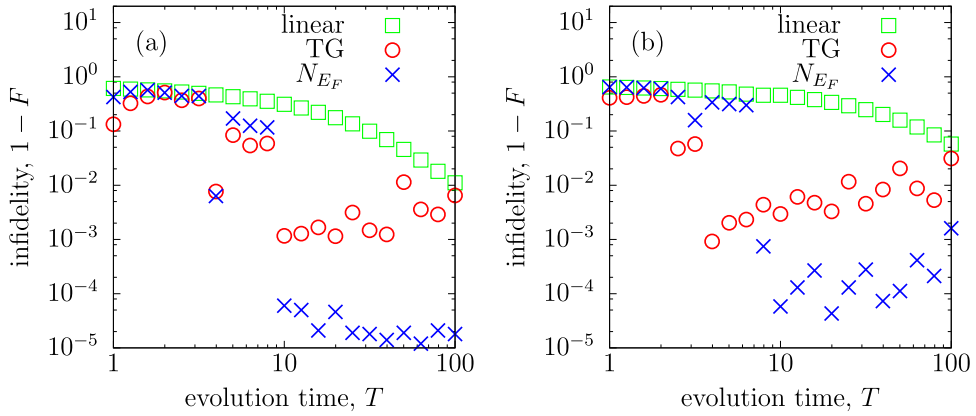

Figure 6. Infidelities for the evolution of a TG gas with (a) $N = 3$ and (b) $N = 5$ particles using the CRAB optimal control technique. The optimal pulses were determined for the particle at the Fermi edge (blue crosses), and applied to the whole gas (green squares). Here, the green squares show the fidelity of a linear pulse for the atom closest to the Fermi edge. A clear range where the CRAB algorithm is effective for generating NOON states with multiple particles can be clearly identified.

4. Shortcuts to adiabaticity

In the following we will discuss the possibility of creating the NOON state by using STA techniques [7]. For this we break the rotational symmetry of the ring system by introducing a time-dependent external potential that we remove again at the end. At variance with the set-up proposed by Hallwood *et al* [3], this scheme can prepare the system in a NOON state without requiring a narrow potential barrier. Instead, we consider the use of a harmonic potential, or a more experimentally realistic sinusoidal potential.

The protocol we suggest consists of five steps, (1) adiabatically raising a weak harmonic potential wrapped around the ring, (2) quickly tightening this potential via a shortcut to localise the particle, (3) accelerating the particle by moving the centre of the harmonic potential via another shortcut, (4) lowering the potential via the reverse process of step (2) to delocalise it again, and (5) adiabatically removing the harmonic potential. A schematic of this process is shown in figure 7. In the next section, we will briefly review the general framework of the STA formalism [7] and detail the differences of our protocol with respect to existing ones.

4.1. Lewis–Riesenfeld invariants

STA methods based on the Lewis–Riesenfeld invariant inverse-engineering approach [18–20] make use of the existence of invariants. A one-dimensional Hamiltonian has an invariant quadratic in momentum p if and only if it can be expressed in the following manner

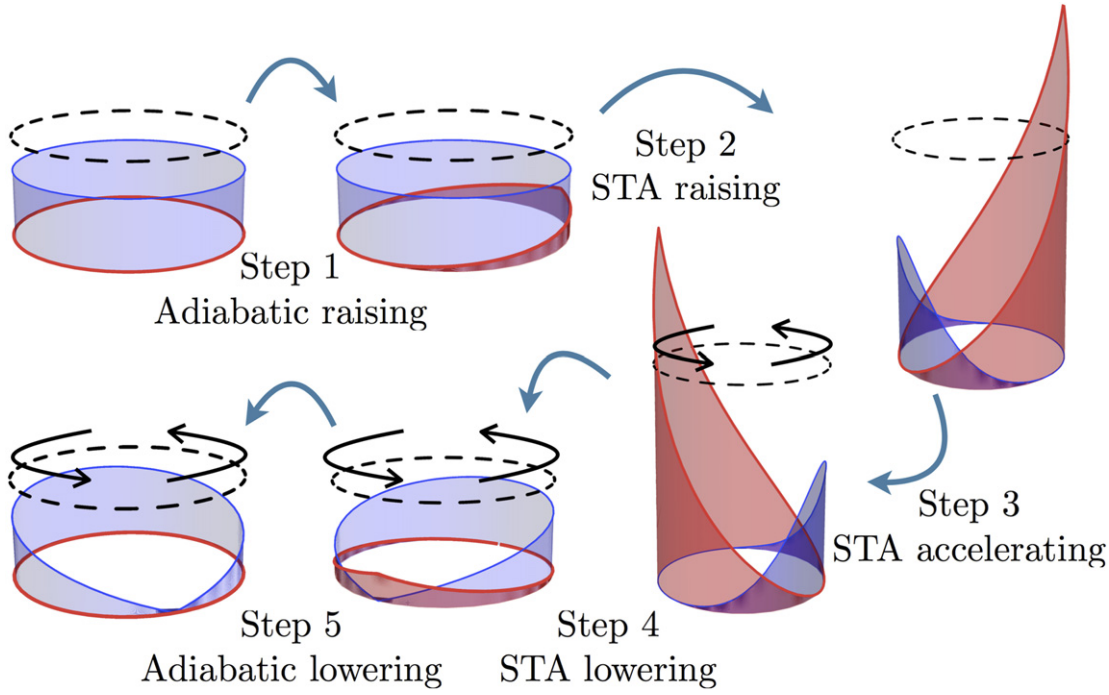

Figure 7. Scheme for the acceleration of a single atom using STA. In this example, the ground state of free space gets localised, accelerated and released at the angular velocity of $\Omega = \pi$ into the state $(\exp(i2\pi x) + 1)/\sqrt{2}$.

$$H = \frac{p^2}{2m} - F(t)q + \frac{m}{2}\omega^2(t)q^2 + \frac{1}{\rho(t)^2}U\left(\frac{q - q_c(t)}{\rho(t)}\right), \tag{11}$$

where U is an arbitrary function and q is the position operator. The variables ρ, q_c, ω, and F are arbitrary functions of time satisfying the auxiliary equations

$$\ddot{\rho} + \omega^2(t)\rho = \frac{\omega_0^2}{\rho^3}, \tag{12}$$

$$\ddot{q}_c + \omega^2(t)q_c = F(t)/m, \tag{13}$$

where ω_0 is a constant. The physical interpretation of the constant and functions depends on the underlying system. Additional constraints have to be considered to insure that the Hamiltonian and its invariants commute at initial and final times t_0 and t_f, which in our case results in $H(t_0) = H(t_f) = p^2/2m$.

4.2. Shortcut for raising/lowering the potential

One of the two shortcuts being used in the protocol above involves raising or lowering of a harmonic potential [19, 21]. For this we only need a stationary harmonic potential and can set F, q_c and U from equation (11) to zero, which leads to

$$H = -\frac{1}{2}\frac{\partial^2}{\partial x} + \frac{1}{2}\omega^2(t)q^2, \tag{14}$$

complemented by the single auxiliary equation (12). To change the frequency from $\omega(t_0) = \omega_0$ to $\omega(t_f) = \omega_f$ while keeping the commutation relations and $\omega(t)$ continuous, we impose the conditions

$$\begin{aligned} &\rho(t_0) = 1, \quad \rho(t_f) = \gamma = \sqrt{\omega_0/\omega_f}, \\ &\dot{\rho}(t_0) = 0, \quad \dot{\rho}(t_f) = 0, \\ &\ddot{\rho}(t_0) = 0, \quad \ddot{\rho}(t_f) = 0. \end{aligned} \tag{15}$$

This means that as long as the conditions (12) and (15) are obeyed, we are free to choose any specific form of ρ. A good choice is a simple polynomial of the form

$$\rho(s) = 6(\gamma - 1)s^5 - 15(\gamma - 1)s^4 + 10(\gamma - 1)s^3 + 1, \tag{16}$$

where $s = (t - t_0)/(t_f - t_0)$, which, when inserted into equation (12), allows us to numerically find a solution for $\omega(t)$. This solution leads to the necessary squeezing or expansion of the particle wavefunction with perfect fidelity in an arbitrarily short time $t_f - t_0$, although in practice a shorter squeezing time involves a faster

variation of ω, which may be limited by technical capabilities. Note that even though this shortcut was not specifically built for systems with periodic boundaries, it can also be used in a ring, as the symmetry of the potential is never broken during the time evolution.

It is also important to note that the initial frequency ω_0 can be chosen arbitrarily small as long as it is non-zero. Furthermore, the solution of equation (12) for very small values of ω_0 can yield purely imaginary values of $\omega(t)$, which corresponds to inverted (repulsive) potentials. While changing potentials between attractive and repulsive is technically possible, such a procedure is often associated with very fast changes with large amplitudes, which may not be easy to realise experimentally. As our final states require the external potential to be absent, i.e. $\omega = 0$, the first step of our protocol raises ω from 0 to a suitable ω_0 adiabatically slowly before the shortcut protocol can be used. In a similar manner, the last step of lowering the potential to $\omega = 0$ after having accelerated the particle has to be done adiabatically.

4.3. Shortcut for the acceleration

Once the potential has been raised, the next step is to accelerate the particles. A shortcut for this process using a harmonic trap exists [22–24], which keeps the trapping frequency constant and only requires a change in the the position of the potential. We can therefore set $U = 0$ and $F = \omega_0^2 x_0(t)$ which leaves

$$H = -\frac{1}{2}\frac{\partial^2}{\partial x} + \frac{1}{2}\omega_0^2(q - x_0(t))^2, \tag{17}$$

and condition (13) becomes the only relevant auxiliary equation

$$\ddot{q}_c + \omega_0^2(q_c - x_0) = 0. \tag{18}$$

We once again impose conditions on q_c such that all boundary conditions are satisfied

$$\begin{aligned} &q_c(t_0) = x_0(t_0), \; q_c(t_f) = d, \\ &\dot{q}_c(t_0) = 0, \qquad \dot{q}_c(t_f) = \Omega_f, \\ &\ddot{q}_c(t_0) = 0, \qquad \ddot{q}_c(t_f) = 0, \end{aligned} \tag{19}$$

where d is the final position of the potential minimum and Ω_f is its final velocity. For transport schemes, d is the important parameter and Ω_f is set to 0, but in our case the opposite occurs as we want the particles to accumulate kinetic energy before being released from the potential (so that they keeps revolving at constant speed Ω_f after t_f). The final position d plays no significant role in the evolution of the states.

The exact form of q_c can again be chosen arbitrarily and we pick the polynomial

$$q_c(s) = (6\,d - 3\Omega_f)s^5 - (15d - 7\Omega_f)s^4 + (10d - 4\Omega_f)s^3 + x_0(t_0), \tag{20}$$

where, as above, s is the normalised time. The value of Ω_f can be chosen as a multiple of 2π to create a plane wave after release, or as an odd multiple of π to prepare superpositions between states of different angular momentum.

Note that this transport scheme is usually applied to an open, infinite space, whereas our system has periodic boundary conditions. Since translational symmetry is broken, the shortcut is no longer guaranteed to work perfectly, as the potential has a finite height and therefore higher-lying states are no longer trapped. Unlike the potential raising shortcut, this accelerating shortcut is only approximate and works best when ω is large (the particle is highly localised) and the rotational velocity, $\dot{q}_c$, is not too high (the harmonic well is not moving too fast).

4.4. Harmonic and sinusoidal potentials

Both shortcuts described above are based on the presence of a harmonic potential of the form

$$V_H(x,\,t) = \frac{1}{2}\omega^2(t)(x - x_0(t))^2, \tag{21}$$

where ω is the frequency of the trap (in units of $\hbar/mL^2$) and x_0 the position of its minimum. Note that we require the potential to be symmetric around x_0 so that the potential is continuous at $x = \pm 1/2$, and therefore the real form of $(x - x_0)$ must be $(x - x_0 + 1/2)(\mathrm{mod}\ 1) - 1/2$. The potential V_H is then continuous everywhere on the ring, but its derivative is discontinuous at $x = x_0 + 1/2$ (the position diametrically opposite to x_0). From a theoretical perspective, V_H is ideal because of its simplicity and its numerous known properties, particularly concerning STA, but it can also be considered a low energy approximation to any experimentally realistic potential. To show that the shortcut approach also works in experimentally realistic potentials, we discuss in the following its application to a sinusoidal potential [25, 26] of the form

$$V_S(x,\,t) = \frac{\omega^2(t)}{2\pi^2}\sin^2(\pi(x - x_0(t))), \tag{22}$$

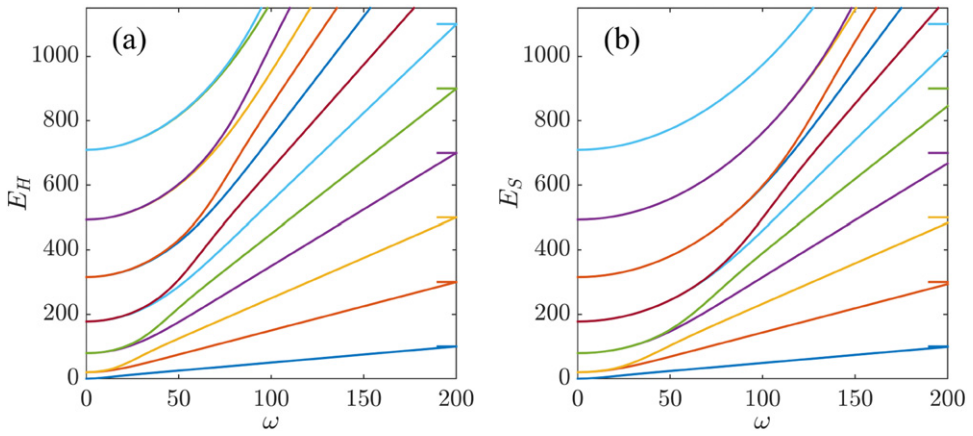

Figure 8. Energy eigenspectrum of the system with (a) a harmonic or (b) a sinusoidal potential as a function of ω. The eigenstates continuously change from angular momentum states of energy $E_k = 2\pi^2 k^2$ (with $k = 0, \pm 1, \ldots$) at $\omega = 0$, towards harmonic-oscillator states of energy $E_n = \omega(n + 1/2)$ (with $n = 0, 1, \ldots$) for large ω. For comparison, the horizontal lines on the right vertical axis give the energy levels in a harmonic potential with $\omega = 200$.

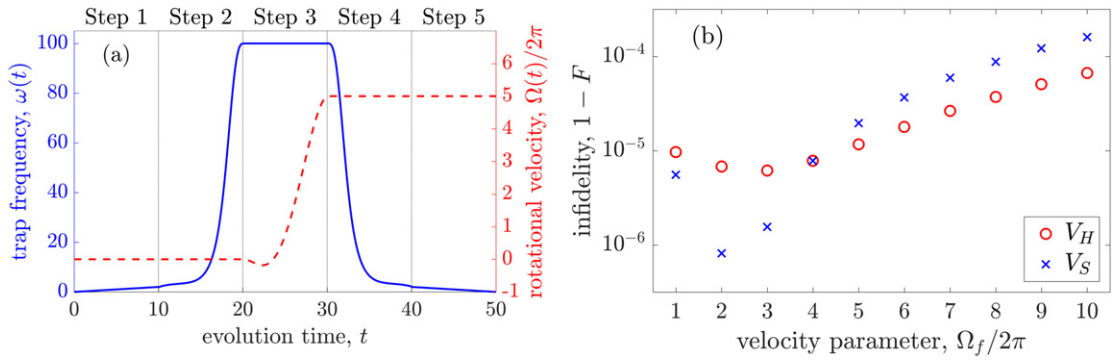

Figure 9. (a) Plot of the parameters $\omega(t)$ and the angular velocity $\Omega(t)$ for the entire protocol. The parameters are $\omega_0 = 2$, $\omega_f = 100$, $d = 100$, each step is executed in $t_f - t_0 = 10$, and Ω_f is picked depending on the desired output state (here, $\Omega_f = 5 \times 2\pi$). (b) Final infidelities for $\Omega_f = 1, 2, \ldots, 10 \times 2\pi$ for V_H (dotted blue line) and V_S (solid red line). The rest of parameters are as shown in (a).

where the notation is the same as before. Note that the pre-factor is chosen in such a way that V_H is an approximation of V_S around x_0.

To visualise the difference between the two potentials, we first compute the energy spectra of both Hamiltonians by using a straightforward discrete variable representation method [27, 28]. The results as a function of ω are shown in figure 8 and one can see that the eigenstates at $\omega = 0$ are the angular momentum states $e^{i2\pi kx}$, with the clockwise and counter-clockwise momentum states of opposite quantum number k being degenerate. The degeneracy is lifted as ω becomes non-zero and the spectrum asymptotically approaches that of a harmonic oscillator. Note that for the sinusoidal case, even for large ω, the difference with the asymptotic harmonic spectrum increases with the quantum number n.

4.5. Single particle acceleration

In the following, we first show the results obtained from numerically simulating our protocol for a single particle initially in the ground state, where the free parameters of the protocol and the lengths of the different steps were chosen to allow for high fidelities. Note that the STA raising/lowering times can in principle be made arbitrarily short for fixed ω_f, unlike the adiabatic or the accelerating steps. In figure 9(a) we show the values for $\omega(t)$ and $\Omega(t)$ which define our chosen protocol, and in figure 9(b) we show the infidelities for the state preparation of plane waves $e^{i\Omega_f x}$ with $\Omega_f = 1 \ldots 10 \times 2\pi$. One can see that the even for a large amount of angular momentum the fidelities remain very high, for both the harmonic and the sinusoidal potential.

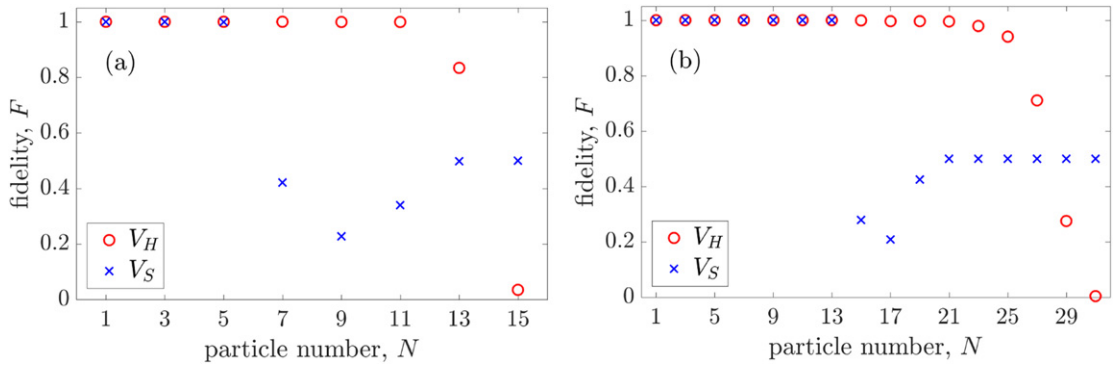

Figure 10. Final fidelities F of TG states of increasing particle number for the protocol shown in figure 9(a) with $\Omega_f = \pi$ for V_H (red circle) and V_S (blue cross). Plot (a) shows the fidelity of the protocol with $\omega_f = 100$ and (b) with $\omega_f = 200$.

4.6. TG gas acceleration

We now consider the multi-particle case in the TG regime. As this protocol does not include a δ-barrier, the target NOON state is slightly different from the one considered in the optimal control case. It corresponds to the state originating from adiabatically removing the barrier once the system is rotating at velocity $\Omega_f = \pi$. Similarly, the initial states for the particles will be eigenstates of free space, which are simply plane waves $e^{i2\pi kx}$ with integer k. Since the states with $\pm k$ are degenerate, however, it is equally valid to consider the initial eigenstates

$$\phi_0^i(x) = 1, \tag{23}$$

$$\phi_{2l-1}^i(x) = \frac{1}{\sqrt{2}}(e^{i2\pi lx} - e^{-i2\pi lx}) = i\sqrt{2}\sin(2l\pi x), \tag{24}$$

$$\phi_{2l}^i(x) = \frac{1}{\sqrt{2}}(e^{i2\pi lx} + e^{-i2\pi lx}) = \sqrt{2}\cos(2l\pi x), \tag{25}$$

for $l = 1, 2, \ldots$. These states have the property of having a total angular momentum of zero and are well suited for our STA protocol. When an odd number of particles occupies the lower eigenstates, the sin/cos pairs are guaranteed to be both populated.

For $\Omega_f = \pi$, the plane wave of quantum numbers $k + 1$ and $-k$ are degenerate and we can construct the target states

$$\phi_{2l}^t(x) = \frac{1}{\sqrt{2}}(e^{i2\pi(l+1)x} + e^{-i2\pi lx}) = \sqrt{2}\cos[(2l+1)\pi x]e^{i\pi x}, \tag{26}$$

$$\phi_{2l+1}^t(x) = \frac{1}{\sqrt{2}}(e^{i2\pi(l+1)x} - e^{-i2\pi lx}) = i\sqrt{2}\sin[(2l+1)\pi x]e^{i\pi x}, \tag{27}$$

for $l = 0, 1, 2, \ldots$. These states, of total angular momentum π, are very similar to the the eigenstates considered in the previous sections and NOON states can be constructed from them.

Any initial state $|\phi_l^i\rangle$ can be brought to the target state $|\phi_l^t\rangle$ (up to a possible shift in position) with high fidelity using our STA protocol. This process also works for TG gases, and we show in figure 10 the fidelity for TG gases of increasing (odd) particle numbers N submitted to our protocol. In figure 10(a) for the harmonic potential, the fidelities remain very high (infidelities of the order of 10^{-4}) for $N \leqslant 11$ after which they decrease. This is due to the finite maximum height of the potential (which, in turn, is due to the periodic boundary conditions), which affects the effectiveness of the STA acceleration scheme. The fidelities can be improved by increasing the maximum trapping frequency ω_f as we demonstrate in figure 10(b) where the value of ω_f is doubled and the fidelities remain high until $N \leqslant 21$. When using the sinusoidal potential, the fidelity drops for smaller particle numbers compared to the harmonic potential (although it also increases with ω_f), due to the lower height V_S has compared to V_H.

5. Conclusion

We have investigated the possibility of creating NOON states with ultracold quantum gases in the TG regime on a ring by using optimal control and STA techniques. Both these techniques were shown to allow to evolve the system into high-fidelity NOON states non-adiabatically.

In the case of optimal control, we used the CRAB technique with the Nelder–Mead minimisation method, for both a single particle and multiple particles by modifying either the potential barrier strength, its rotational velocity, or both. In all cases NOON states can be generated in finite time and with high fidelity. In particular, we have shown that it is sufficient to optimise for the particle closest to the Fermi edge to achieve high TG fidelities. In a second approach, we have generalised two known STA techniques to a ring system, and shown that STA techniques may also be used to create rotational states with high fidelity for both single particles and strongly correlated TG gases. The STA protocol we have applied is composed of five steps, where only the first and final steps required adiabaticity. Thus we have demonstrated that it is also possible to implement STA techniques on a one-dimensional ring system and generate NOON states between ultracold bosons without a potential barrier in the end.

The results presented here clearly show that it is possible to create macroscopic superposition states in TG gases on experimentally realistic timescales. They may therefore lead to a method of generating NOON states on a ring of ultracold atoms for use in quantum information systems.

References

[1] Israel Y, Afek I, Rosen S, Ambar O and Silberberg Y 2012 *Phys. Rev.* A **85** 022115
[2] Afek I, Ambar O and Silberberg Y 2010 *Science* **328** 1188172
[3] Hallwood D, Ernst T and Brand J 2010 *Phys. Rev.* A **82** 063623
[4] Girardeau M 1960 *J. Math. Phys.* **1** 516
[5] Hallwood D, Burnett K and Dunningham J 2007 *J. Mod. Opt.* **54** 2129–48
[6] Caneva T, Calarco T and Montangero S 2011 *Phys. Rev.* A **84** 022326
[7] Torrontegui E, Ibáñez S, Martínez-Garaot S, Modugno M, del Campo A, Guéry-Odelin D, Ruschhaupt A, Chen Xi and Muga J G 2013 *Adv. At. Mol. Opt. Phys.* **62** 117–69
[8] Das K K, Girardeau M D and Wright E M 2002 *Phys. Rev. Lett.* **89** 170404
[9] Girardeau M D and Minguzzi A 2009 *Phys. Rev.* A **79** 033610
[10] Girardeau M D, Wright E M and Triscari J M 2001 *Phys. Rev.* A **63** 033601
[11] Girardeau M D and Wright E M 2000 *Phys. Rev. Lett.* **87** 050403
[12] Shenke C, Minguzzi A and Hekking F 2012 *Phys. Rev.* A **85** 053627
[13] Nunnenkamp A, Rey A M and Burnett K 2008 *Phys. Rev.* A **77** 023622
[14] Nelder J and Mead R 1965 *Comput. J.* **7** 308–13
[15] Martínez-Garaot S, Ruschhaupt A, Gillet J, Busch T and Muga J G 2015 *Phys. Rev.* A **92** 043406
[16] del Campo A 2011 *Phys. Rev.* A **84** 012113
[17] Lelas K, Ševa T and Buljan H 2011 *Phys. Rev.* A **84** 063601
[18] Lewis H R and Riesenfeld W B 1969 *J. Math. Phys.* **10** 1485
[19] Chen X, Ruschhaupt A, Schmidt S, del Campo A, Guéry-Odelin D and Muga J G 2010 *Phys. Rev. Lett.* **104** 063002
[20] del Campo A and Boshier M G 2012 *Sci. Rep.* **2** 648
[21] Chen X and Muga J G 2010 *Phys. Rev.* A **82** 053403
[22] Masuda S and Nakamura K 2010 *Proc. R. Soc.* **466** 1135–54
[23] Torrontegui E, Ibáñez S, Chen X, Ruschhaupt A, Guéry-Odelin D and Muga J G 2011 *Phys. Rev.* A **83** 013415
[24] Masuda S 2012 *Phys. Rev.* A **86** 063624
[25] Phelan C F, Hennessy T and Busch T 2013 *Opt. Express* **21** 27093–101
[26] Masuda S, Nakamura K and del Campo A 2014 *Phys. Rev. Lett.* **113** 063003
[27] Light J C and Carrington T 2000 *Adv. Chem. Phys.* **114** 263–310
[28] Baye D and Heenen P H 1986 *J. Phys. A: Math. Gen.* **19** 2041